CHAPTER 4

INTERACTION OF CHLORIN P_6 WITH SINP-VA: PHOTOPHYSICAL AND PHOBIOLOGICAL STUDIES

In this chapter we present the results our investigations on interaction of Chlorin p_6 (Cp_6) with silica nanoparticles having positively charged amino groups (SiNP-VA). The effect of binding between the drug and SiNP-VA on the acid-base ionization equilibrium of Cp_6 is described in detail by studying its absorption and emission properties in aqueous medium. Results of fluorescence correlation spectroscopy and photostability of Cp_6 and Cp_6-SiNP-VA complex, in the presence of serum are also provided. Finally, we present a comparative study on cellular uptake, intracellular localization and phototoxicity between free Cp_6 and Cp_6-SiNP-VA complex in cancer cell lines.

Work discussed in this chapter resulted in the following publication:

1. 'Spectroscopic investigations on the binding of the photosensitizer Chlorin p_6 with amine modified silica nanoparticles in aqueous media' B. Jain, A. Uppal, P. K. Gupta and K. Das, *Photochemistry and Photobiology*, Vol. 85, pp. 927-933 (2009).
2. 'Evaluation of photodynamic efficacy of Chlorin p6 bound to amine modified silica nanoparticles in Colon and Oral cancer cell lines', A. Uppal, B. Jain, M. K. Swami, H. S. Patel, A. Dube, P. K. Gupta and K. Das, In press, *BioNanoScience.*

4.1 Introduction

Cp_6 is one of the chlorophyll-a derivatives. It is amphiphillic in nature and is negatively charged at physiological pH. Previous in vitro and in vivo studies have shown that Cp_6 possess promising photodynamic properties [130]. Studies carried out in our group on breast and colon carcinoma cells have shown that PDT with Cp_6 primarily cause damage to lysosomes and mitochondria depending on the pH of the extracellular medium [131]. In the hamster cheek pouch model, Cp_6 showed preferential accumulation in small tumors (< 5 mm) resulting in complete tumor necrosis and regression after PDT, however, the accumulation of Cp_6 in relatively larger tumor was poor [132].

Recently, the use of NPs for improving delivery of photosensitizer in tumor has received considerable attention due to the fact that compared to small drug molecules, the retention of large size nanoparticles in tumor tissue is more due to the enhanced permeability and retention effect (EPR) [133]. However, conjugation of photosensitizer to nanoparticles can lead to substantial changes in the photophysical and photochemical properties, which can also modulate its photodynamic efficacy/phototixicity as it is shown in the case of MC540 (chapter 3). Since SiNP-VA contains 3-amino propyl groups which are positively charged at physiological pH (chapter 3), these can be used to electrostatically bind to this negatively charged photosensitizer, Cp_6.

Cp_6 has three ionizable carboxylic acid groups. Different ionic structures involving protonation-deprotonation of the three carboxylic acid groups of the molecule as a function of pH are depicted in Fig. 4.1. It is pertinent to note that the sequence of the structures shown is only notional. The pH dependent acid-base equilibrium of Cp_6 has been studied by absorption and fluorescence spectroscopy [91]. It has been observed that at physiological pH the dye exists predominantly as negatively charged (i.e. closer to structure D in Fig. 4.1) and as the pH is progressively lowered, successive protonation of the carboxyl groups (forming structures C to A in Fig. 4.1) results in aggregation of the dye in aqueous medium.

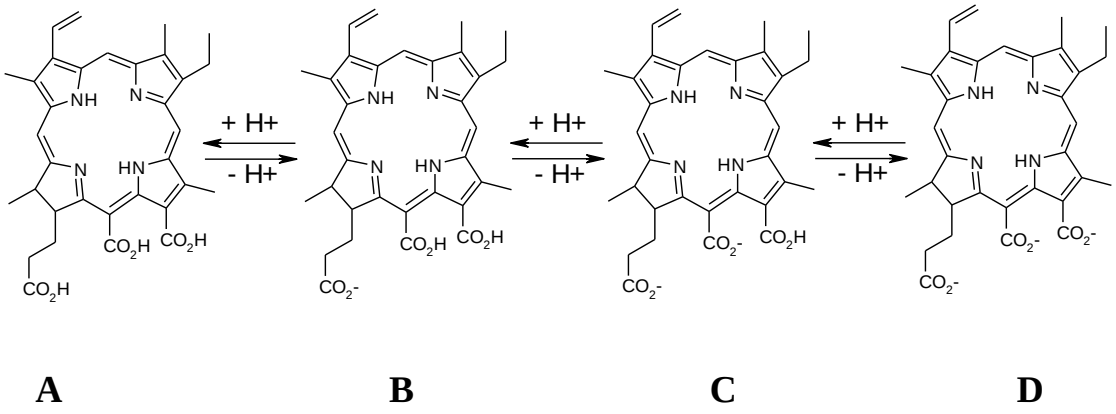

Figure 4.1 *Different ionic structures of* C*p*$_6$ *possible in the pH range of 3-8.*

The hydrophobic aggregates have been observed to be nonfluorescent [91]. It has been observed that, by controlling the relative populations of the species A-D, pH plays an important role in the relative binding of the dye with various systems like micelles, liposomes, proteins and biopolymers [91, 134135136137138]. Indeed it was observed that with a decrease in the pH of the incubation medium (from 7.4 to 6.0) the uptake of the dye increased in human colon adenocarcinoma (Colo-205) cells [131]. Further, it has also been observed that the electrostatic binding of the dye with charged surfactants can affect the ionization equilibrium of the dye in aqueous medium [134, 135]. Thus, it is to be expected that electrostatic binding with charged silica nanoparticles (SiNPs) would affect its acid/base ionization equilibrium and thus cellular uptake.

To investigate this aspect, we have studied the acid-base ionization equilibrium of C*p*$_6$ in the presence of SiNP-VA (SiNP) by monitoring the spectroscopic (absorption and fluorescence) properties of the dye. We further investigated the effect of conjugation of C*p*$_6$ with these SiNPs on its cellular uptake, its localization in the cells, photostability and phototoxicity in colon and oral cancer cell lines. We observed that the phototoxicity due to C*p*$_6$-SiNP complex was higher than free C*p*$_6$. Possible reasons for this are also addressed.

4.2 Experimental Details

Cp_6 was synthesized in house following the procedure described in reference 5. All the solvents used were spectroscopic grade. SiNP-VA was synthesized as described in chapter 2. The concentration of Cp_6 was fixed at 1 μM for absorption and emission experiments. The pH of the aqueous medium was varied between 3.0 and 8.0 by adding microliter amounts of 1(N) HCl or NaOH. Experiments were not conducted below pH 3.0 as it resulted in nanoparticle aggregation and not above pH 8.0 to ensure that all the 3-amino propyl groups on the surface of the SiNP-VA (SiNP) remain positively charged to bind the dye. Emission lifetimes of Cp_6 were recorded by excitation at 406 nm using a picosecond diode laser as described in chapter 2 [136].

In order to investigate the relative association of the Cp_6 with serum proteins and SiNP, fluorescence correlation spectroscopy (FCS) experiments were performed in presence of SiNP with varying amounts of serum. The details of the setup are given in chapter 2, section 2.2.2. In all the measurements the SiNP and Cp_6 concentration was kept same (200 μgm/mL and 10μM respectively) and the serum concentration was varied from 2.5-10%. The emission was monitored at 670 nm.

For cellular studies, Colon cancer cells (Colo-205) and human squamous cell (oral) carcinoma cell line Nt8e were obtained from National Centre for Cell Sciences, Pune, India and Advanced Centre for Treatment, Research and Education in Cancer (ACTREC), Mumbai, India respectively. Experimental samples for cellular studies were prepared by Dr. A. Uppal. Briefly, the cells were grown in monolayer at 37^{o}C in humidified incubator (RS Biotech, UK) under 5% CO_2 – 95% air atmosphere. The cells were harvested by trypsinization, re-suspended in culture media and plated in either microplate wells or 35 mm Petri dishes after adjusting the cell number by counting in a haematocytometer.

The cellular uptake of the Cp_6 and Cp_6-nanoparticle complex was estimated by fluorescence spectroscopy. For this a growth medium containing free Cp_6 or Cp_6-SiNP

was added to the exponentially growing cells in 35 mm petri dishes and the cells were incubated at 37^{o} C under 5% CO_2 – 95% air atmosphere in dark for 3 hour. Subsequent to incubation, the culture medium containing the photosensitizer or its complex with SiNP was removed and the cell monolayer was washed three times with cold PBS. The cells were harvested by trypsinization, centrifuged at 600 g for 10 minutes and then re-suspended in PBS.

The cellular uptake of the Cp_6 was initially measured in the cell suspension and then counter checked in the cell extract also to check for the possible interference of the cellular environment on the fluorescence measurements. For both the measurements, the excitation wavelength was centered at 400 nm (corresponding to the Soret band absorption peak of Cp_6) and the fluorescence emission was scanned from 600-750 nm. In case of cell suspension, the relative amount of the Cp_6 was estimated from the value of fluorescence intensity at 670 nm (corresponding to the fluorescence maxima of Cp_6) after normalization with respect to the cell number. For estimations in the cell extracts, the cell monolayer treated with Cp_6 was washed thrice with PBS to remove extracellular Cp_6, and then a solution of 0.1 N NaOH and 0.1% SDS was added to lyse the cells. The cell lysate was pipetted several times to give a homogenous solution followed by centrifugation at 600 g for 10 min. The supernatant was mixed with PBS to a final volume of 2.0 ml and used for fluorescence measurements as described above. The cellular uptake of Cp_6 was quantified from the relative fluorescence intensity at 670 nm after normalizing with respect to the protein content in the cell extract as measured by Lowry's method [139].

To visualize the intracellular localization of the Cp_6, the cells were grown on gelatin coated cover slips and incubated with either free Cp_6 or Cp_6-SiNP in a growth medium at 37° C in dark for 3 hour. After incubation, the cover slips were washed thrice with cold PBS and then observed under an inverted microscope (Olympus IX70) using fluorescence filter set (excitation 530–560 nm, barrier filter 580 nm). The images were

recorded using a CCD Camera (ProgRes C Fscan) and ProgRes Capture Pro software (Jenoptik, Germany).

For phototoxicity experiments, cells were grown in a 96 well standard microplate and incubated with Cp_6 or Cp_6-SiNP complex in growth medium for 3 h at 37° C in dark. After incubation, the growth media containing Cp_6 was removed and the monolayer was washed with culture medium containing no serum. Cells were placed in fresh growth medium and then exposed to red light (660 ± 20 nm) using an LC-122A light source (CI TEK, USA) and an optical fiber probe (diameter 1.2 cm, length 1 m) that had an in-built band-pass filter. The optical fiber probe was kept at a height of ~ 14 cm from the microplate to produce an illuminated area of diameter ~19 cm. The power density at the level of microplate was ~9mW/cm^2, as measured by a power sensor 3A-P (Ophir). For homogenous illumination (power variation <5%) of the wells, the microplate was kept in the centre of this area and to ensure that there is no crosstalk between wells, the distance between the two samples was kept at least two rows apart. During irradiation, all the wells were covered with a black paper except the wells to be irradiated. Two separate plates were used for dark control and for light irradiation to avoid light exposure to dark control samples. Phototoxicity was assessed by MTT assay as described in chapter 2, [102]. Percent cell survival in all the samples was calculated with respect to the value obtained in the control sample. All the cell experiments were repeated at least three times and data obtained are presented as average and standard deviation (n = 3). The significance of the difference between the treatments was analyzed by student's t test.

To investigate possible photobleaching of the Cp_6 and Cp_6-nanoparticle complex due to red light irradiation (660 ± 20 nm, 28 mW/cm^2), the absorbance spectra of both were recorded at time intervals of one minute over a seven minutes photoirradiation period. The kinetics was followed by monitoring the decrease in the Soret band (400 nm) absorbance of Cp_6.

4.3 Results

4.3.1 Effect of SiNP on the absorption and emission of Cp_6 from pH 8.0 to 3.0

The absorption and emission properties of Cp_6 are found to dependent on the pH of the aqueous media as shown in Fig. 4.2. As the pH decreases a considerable decrease in the absorption intensities of the Soret and Q band (around 400 and 655 nm respectively at pH 8.0) are observed (Fig. 4.2a). In addition the Q band also shows a blue shift to 642 nm and below pH 5.0, it splits into two bands (640 & 665 nm) with a further decrease in the

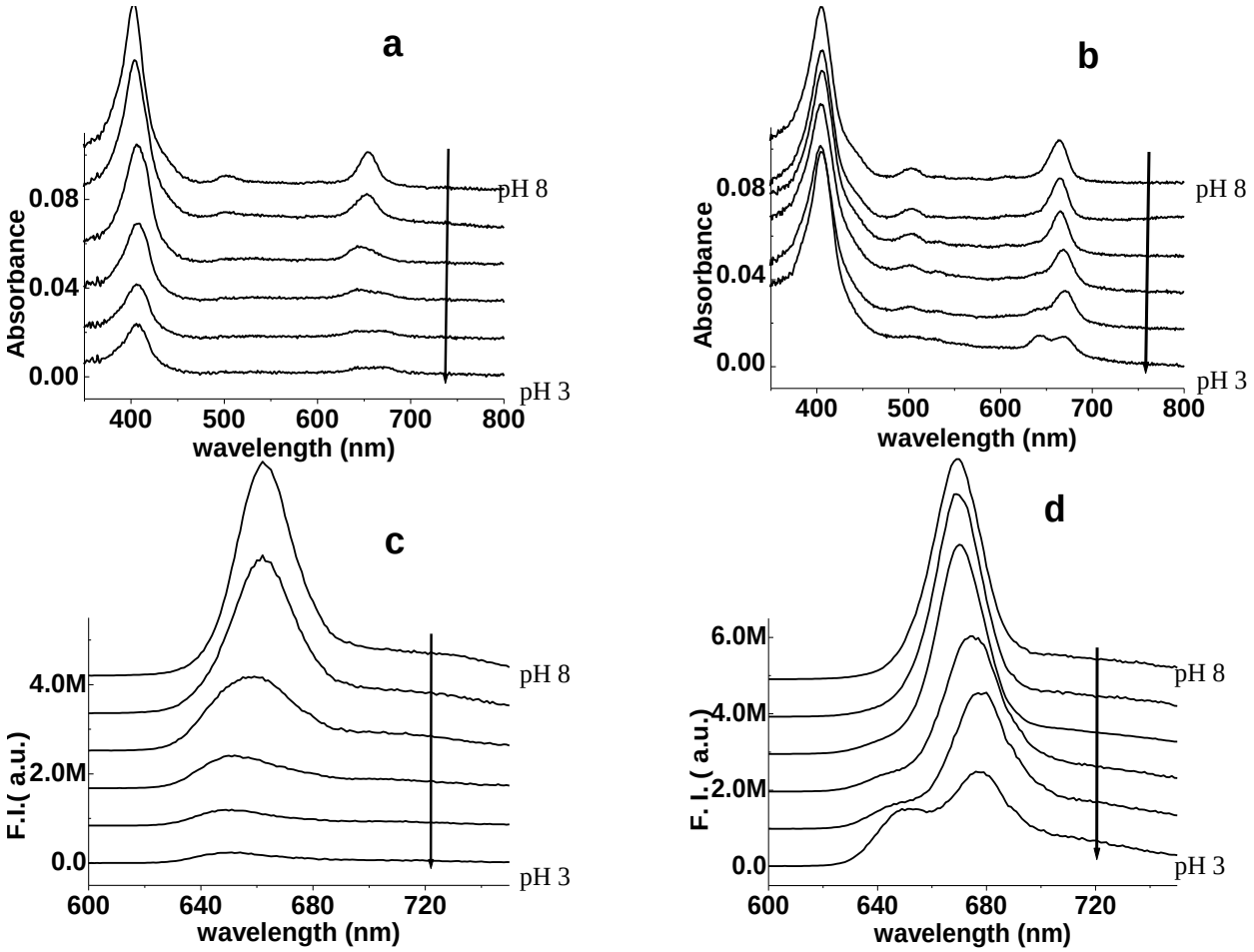

Figure 4.2 *Absorption (top b) & emission (bottom d) spectra of Cp_6 in the presence of 940 µgm/mL SiNP at different pH. (The corresponding spectra without SiNP is given in the left side panel a and c) The arrow represents the increase in pH from 3 to 8 in steps of unity. Although the spectra are shown in same Y-axis scale, they are shifted vertically for clarity.*

intensity. The emission from the dye (excited at 400 nm) decreases by ~12 times with a progressive blue shift of the band from 662 nm to 650 nm as the pH is lowered from 8.0 to 3.0 (Fig. 4.2c). These observations are consistent with the results of a previous study [91]. In the presence of SiNPs, as described in Fig. 4.2b and d, this pH dependent absorption and emission properties of the dye gets considerably modified. In the absorption spectra, the change in the intensities of the Soret and Q band region is modest, however, a red shift of the latter is observed (from 655 nm to 665 nm). Below pH 5.0, the Q band splits into two bands having maxima at ~670 and ~640 nm respectively. The emission of the dye in the presence of SiNPs is red shifted from 662 nm to 670 nm (at pH 8.0) and decreases to a much lesser extent (~ 1.3 times) as the pH is lowered. In addition it splits into two peaks having maxima at 650 and 678 nm of which the appearance of the latter starts becoming prominent below pH 6.0.

The pH dependent absorption and emission parameters of the dye in the presence and absence of SiNPs are given in Table 4.1 for comparison. In order to gain more insight about how the pH dependent spectroscopic properties of the dye gets modulated in the presence of nanoparticles we have carried out a fluorescence titration of the dye with varying SiNP concentration at pH 8.0, 5.0 and 3.0 was carried out, the results of which are described in the next sections.

Table 4.1 *Absorption & emission parameters of Cp_6 at different pH in the presence and absence of SiNP*

pH	Absorption maxima (Q-band)		Emission maxima (λ_{ex} = 400 nm)		Normalized integrated emission intensity[a]	
	No SiNP	SiNP	No SiNP	SiNP	No SiNP	SiNP
8	655	665	662	670	1.00	1.08±0.02
7	652	665	662	670	0.82±0.02	1.09±0.04
6	645	665	660	670	0.51±0.03	1.06±0.04
5	642	668	652	675[b]	0.23±0.02	0.98±0.03
4	640 & 665	670 & 640	650	678[b]	0.11±0.03	0.92±0.03
3	640 & 665	668 & 642	650	678 & 650	0.08±0.02	0.84±0.05

[a]*Normalized with respect to that in water at pH 8.0*

[b]*Although two peaks are not prominent, the presence of a shoulder is observed around 650 nm*

Fluorescence titration of Cp_6 with SiNP at pH 8.0:

The fluorescence properties of the dye were observed to change significantly with addition of SiNP at pH 8.0 where the tri-anionic form of the dye (species D, Fig. 4.1) is expected to be present. Fig. 4.3 describes the change in the fluorescence properties of the dye with increasing amounts of SiNP added at pH 8.0. Fig. 4.3a shows the fluorescence spectra of the dye for selected SiNP concentrations. Fig. 4.3b shows the normalized integrated emission intensity and average lifetimes of the dye against increasing SiNP concentration. The lifetimes of the dye in the absence and in the presence of maximum amount of SiNP used in this study are also shown in Fig. 4.3a (inset) for comparison. With increasing amounts of SiNP, the fluorescence intensity as well as lifetime of the dye decreases initially and reach to a minimum at a SiNP concentration of 19.0 µgm/mL. After that, both fluorescence intensity and lifetime increases steadily with a red shift of the band peak (from 662 nm to 670 nm). Table 4.2 summarizes the emission and lifetime parameters of the dye at various SiNP concentrations at three pHs.

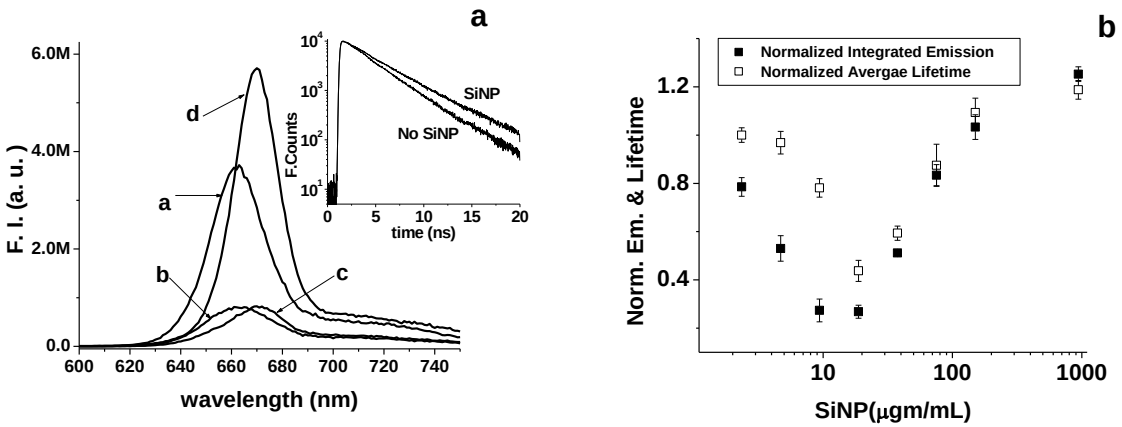

Figure 4.3 ***(a)*** *Fluorescence titration (λ_{ex} = 400 nm) of Cp_6 with increasing amounts of SiNP at pH 8. a) 0 µgm/mL; b) 9.4 µgm/mL; c) 18.8 µgm/mL and d) 940 µgm/mL of SiNP.* ***(Inset)*** *Fluorescence decays (λ_{ex} = 406 nm, λ_{em} monitored at 665 ± 4 nm) of Cp_6 in the presence and absence of 940 µgm/mL of SiNP.* ***(b)*** *Normalized integrated emission and normalized average lifetime of Cp_6 with increasing SiNP. The values are normalized with respect to that of the dye in the absence of SiNP.*

Fluorescence titration of Cp_6 with SiNP at pH 5.0.

When the pH of the medium is decreased from 8.0 to 5.0, partial protonation of the carboxyl groups occurred resulting in aggregation of the dye and thereby causing its fluorescence intensity to decrease by ~4 times accompanied by a noticeable blue shift of the fluorescence maxima (Table 4.1). Fig. 4.4 describes the effect of the addition of increasing amounts of SiNP on the fluorescence properties of the dye at this pH. Figure 4.4a shows the fluorescence spectra of the dye for selected SiNP concentrations. In Fig. 4.4b, results of fluorescence titration of the dye with SiNP are plotted against the normalized integrated emission intensity and average lifetimes of the dye are shown.

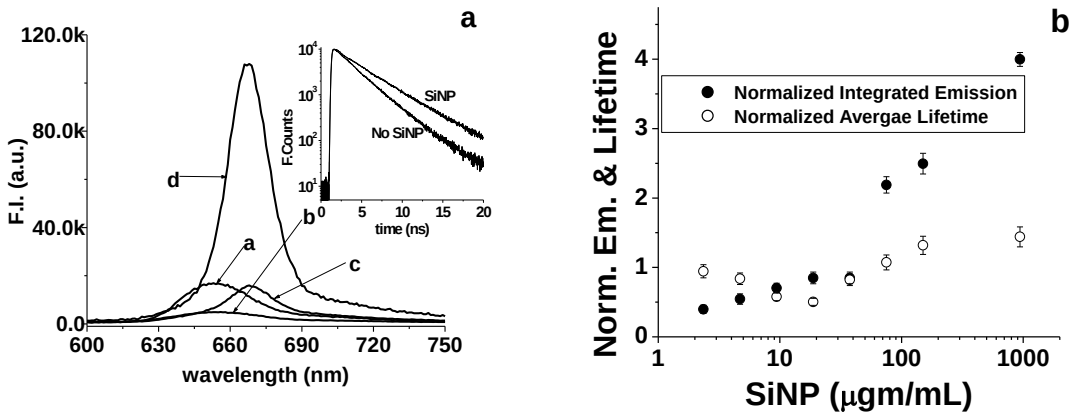

Figure 4.4 ***(a)*** *Fluorescence titration (λ_{ex} = 400 nm) of Cp_6 with increasing amounts of SiNP at pH 5.0: a) 0 µgm/mL; b) 9.4 µgm/mL; c) 18.8 µgm/mL and d) 940 µgm/mL of SiNP. (**Inset**) Fluorescence decays (λ_{ex} = 406 nm) of Cp_6 in the presence (monitored at 675 ± 4 nm) and absence (monitored at 650 ± 4 nm) of 940 µgm/mL of SiNP at pH 5.0.* ***(b)*** *Normalized integrated emission and normalized average lifetime of Cp_6 with increasing SiNP at pH 5.0. The values are normalized with respect to that of the dye in the absence of SiNP. The X-axis is represented in the log scale for clarity.*

Unlike pH 8.0, the normalized integrated fluorescence intensity does not have a steep minimum over the concentration ranges of SiNP used because the minimum occurs as soon as SiNPs are added (2.35 µgm/mL). After that the fluorescence intensity increases steadily with a 23 nm red shift of the band (from 652 nm to 675 nm observed at a SiNP concentration of 37.6 µgm/mL). The average lifetime have a minimum around SiNP

concentration of ~19.0 µgm/mL and then increases steadily. The emission and lifetime of the dye at various SiNP concentrations at this pH are summarized in Table 4.2.

Fluorescence titration of Cp_6 with SiNP at pH 3.0:

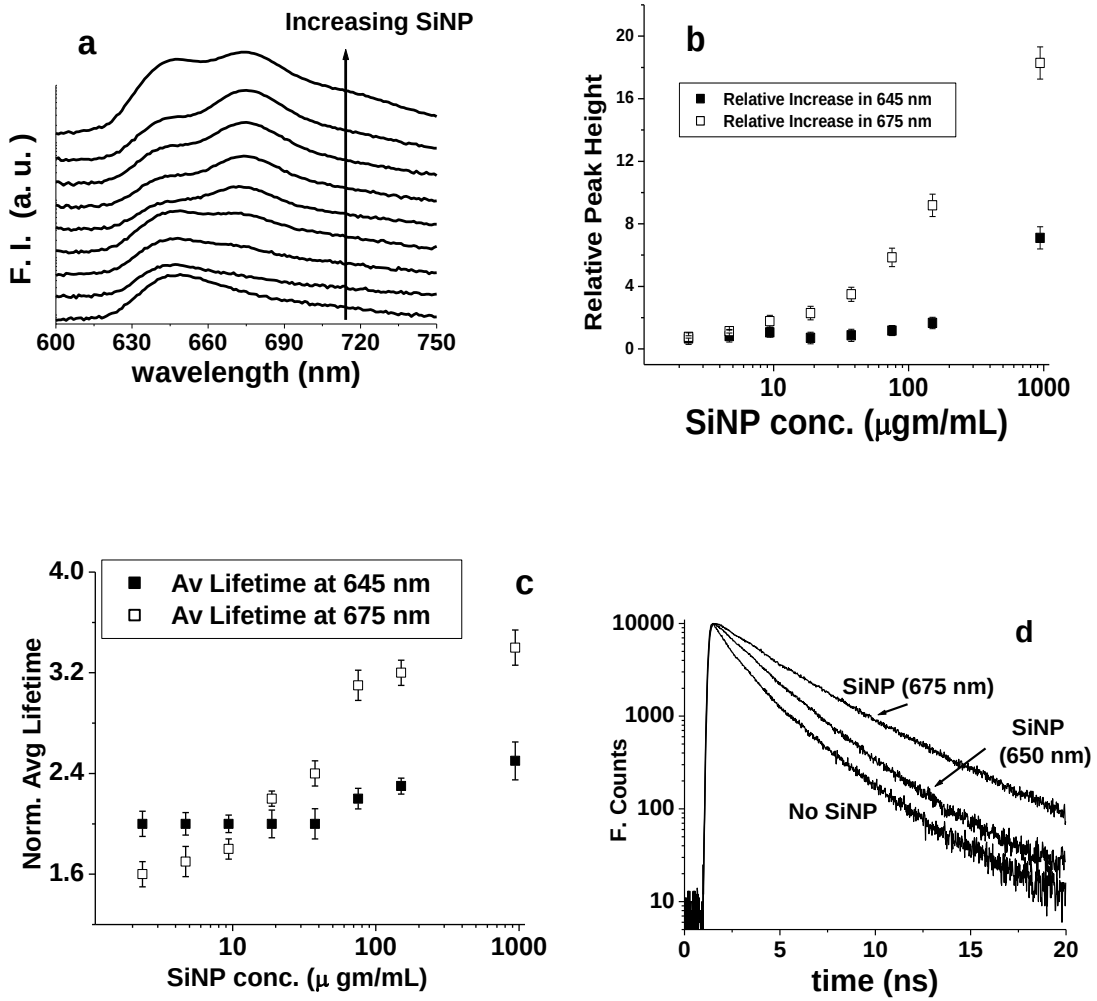

Figure 4.5 ***(a)*** *Fluorescence titration (λ_{ex} = 400 nm) of Cp_6 with increasing amounts of SiNP at pH 3.0. The arrows represent increasing SiNP concentration (from 0 to940 µgm/mL). The spectra are shifted vertically for clarity.* ***(b)*** *Relative change in the fluorescence intensity (λ_{ex} = 400 nm) of the dye monitored at 650 and at 675 nm upon addition of SiNP. The values plotted are normalized relative to that in pH 3.0 solution.* ***(c)*** *Relative change in the fluorescence lifetime (λ_{ex} = 406 nm) of the dye monitored at 650 and at 675 nm upon addition of SiNP. The values plotted are normalized relative to that in pH 3.0 solution.* ***(d)*** *Fluorescence decays (λ_{ex} = 406 nm) of Cp_6 in the presence (monitored at 678 ± 4 nm & 650 ± 4 nm) and in absence (monitored at 650 ± 4 nm) of 940 µgm/mL of SiNP at pH 3.0.*

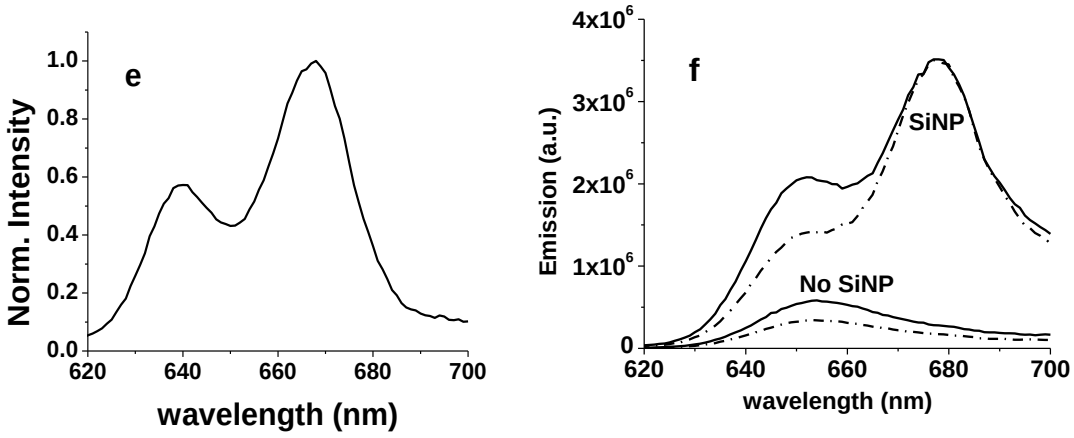

Figure 4.5 (e) *Synchronous fluorescence spectra of Cp_6 in the Q-band region in the presence of 940 µgm/mL of SiNP at pH 3.0 (offset between excitation & emission = 10 nm).* ***(f)*** *Effect of 0.9 (M) acrylamide on the fluorescence of Cp_6 (λ_{ex} = 400 nm) in the presence and absence of SiNP (940 µgm/mL). Dashed lines denote the fluorescence in presence of the quencher.*

When the pH of the medium is further decreased to 3.0 causing further protonation of the carboxyl groups, enhanced aggregation accompanied by a significant quenching (~12 times) of the dye's fluorescence takes place without SiNPs as shown in Table 4.1. At this pH the fluorescence properties of the dye are observed to change differently with addition of SiNP than that observed at pH 8.0 and 5.0. Fig. 4.5a shows how the fluorescence of the dye changes with increasing amounts of SiNP. The fluorescence of the dye shows dual emission centered at 650 and 678 nm, the intensity of the latter increases progressively with the SiNP. A plot of the peak intensities and lifetimes monitored at 650 and 678 nm is shown in Fig. 4.5b & c. It is clear from these figures that the emission intensities and lifetimes at 650 nm do not change very much (except near the highest SiNP concentration), whereas they change significantly when monitored at 678 nm. The lifetimes of the dye at various SiNP concentrations at this pH are given in Table 4.2. Fig. 4.5d shows the variation in the lifetime of the dye (monitored at 650 and 675 nm) in the presence and absence of maximum amount of SiNP. In order to ascertain the origin of the two emission bands at this pH, a synchronous fluorescence scan of the dye was performed in the presence of maximum amount of SiNP.

Table 4.2 *Relative integrated emission intensity and average lifetimes of Cp_6 with various amount of SiNP at pH 8.0, 5.0 and 3.0*[a]

SiNP (µgm/mL)	pH 8.0		pH 5.0		pH 3.0[c]	
	Integrated emission	[b]Average lifetime at 665 nm	Integrated emission	[b]Average lifetime at 675 nm	[b]Average lifetime at 650 nm	[b]Average lifetime at 675 nm
0	1	3.2±0.2	1	2.7±0.3	2.0±0.2	- d-
2.35	0.79±0.04	3.2±0.2	0.40±0.06	2.6±0.2	2.0±0.1	1.6±0.1
4.7	0.53±0.05	3.0±0.1	0.54±0.07	2.3±0.1	2.0±0.3	1.7±0.1
9.4	0.27±0.05	2.2±0.2	0.70±0.07	1.6±0.2	2.0±0.1	1.8±0.2
18.8	0.27±0.03	1.1±0.1	0.85±0.08	1.4±0.1	2.0±0.2	2.2±0.1
37.6	0.51±0.01	1.8±0.3	0.85±0.08	2.2±0.3	2.0±0.1	2.4±0.3
75.2	0.83±0.04	2.9±0.1	2.19±0.11	2.9±0.4	2.2±0.3	3.1±0.2
150.4	1.03±0.05	3.5±0.2	2.50±0.15	3.6±0.2	2.3±0.2	3.2±0.1
940	1.25±0.03	3.9±0.4	4.00±0.10	3.8±0.3	2.5±0.4	3.5±0.1

[a]*For each pH, the integrated emission intensities are normalized against the zero SiNP*
[b]*The lifetimes of the dye in most cases can be fit satisfactorily with two exponentials; however for some cases a three exponential fit is required. All the lifetimes (given in nanoseconds) reported here are average lifetimes. For pH 5.0, in the absence of SiNP, the average lifetime was monitored at 650 nm.*
[c]*For pH 3.0, only the lifetimes are given.* [d]*Not measured.*

Observation of two peaks at ~645 and ~670 nm in Fig. 4.5e suggests the possibility of two species of the dye being present at this pH in the presence of SiNP. To investigate this aspect further, we studied the effect of a quencher, acrylamide, on the dye's fluorescence in the presence and absence of SiNP. The results are presented in Fig. 4.5f. A 40 % quenching of the dye's fluorescence was observed at an acrylamide concentration of 0.9 M indicating that the dye in aqueous environment is accessible to the quencher. However, in the presence of SiNP, only the fluorescence band centered at 650 nm showed significant quenching implying that the species emitting at this wavelength is accessible to the quencher and therefore is most likely to be the free dye present in the aqueous environment.

In order to check whether Cp_6 remain accociated with SiNP in cellular medium, the relative association of the Cp_6 with serum proteins and SiNP was investigated, as

serum forms a major component of cell culture, by performing FCS experiments with varying amounts of serum at pH 7.4.

4.3.2 FCS studies of the free Cp_6 and Cp_6-SiNP complex

The results of the FCS experiments are shown in Fig. 4.6.

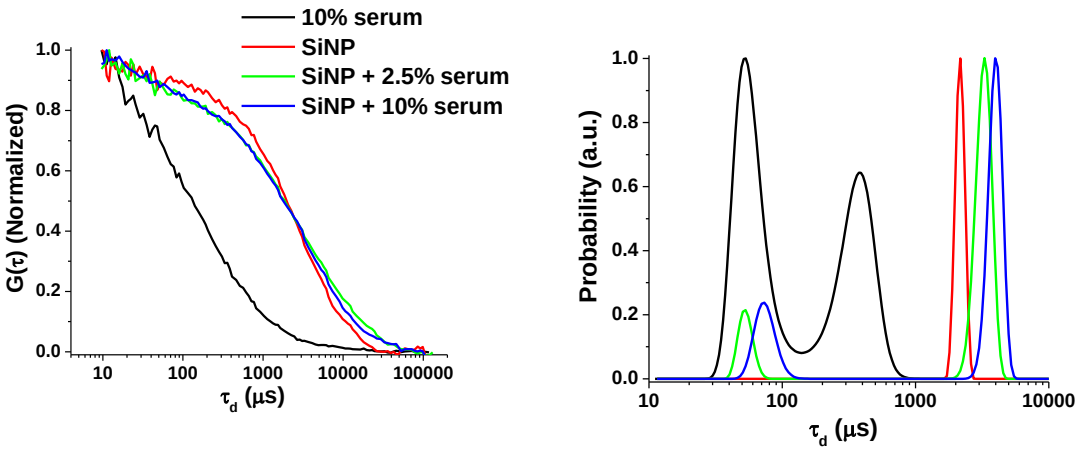

Figure 4.6 *Autocorrelation traces (left) and their fits (right) of 10 µM Cp$_6$ in various environments.*

The left panel describes the autocorrelation traces of the Cp_6 in presence of only SiNP, only 10% serum and two different mixtures of SiNP and serum where SiNP concentration is kept constant (*200 µgm/mL)*and the serum concentration was kept as 2.5 and 10%. The corresponding fits to the traces are shown in the right panel of Fig. 4.6. Three typical diffusion times are obtained from the fits which may be attributed to the free Cp_6 (40-70 µsec), Cp_6 bound to serum (380 µsec) and Cp_6 bound to SiNP (2000-4000 µsec). The figure shows significantly higher probability of Cp_6 bound to SiNP even in the presence of serum proteins at all the concentrations used in the experiment and even at 10% serum concentration which is similar to that used for the uptake and toxicity experiments.

4.3.3 Intracellular uptake, localization and phototoxicity of free Cp_6 and its SiNP complex

Intracellular uptake: The results of the fluorescence measurements on intracellular uptake of Cp_6 and its SiNP complex in Colo-205 and NT8e cells at two different concentrations (5 and 10 µM of Cp_6 alone and its complex with 100 and 200 µg/ml SiNP, respectively at pH 7.4) are shown in Fig. 4.7a & b. The Cp_6 fluorescence was measured in intact cells as well as in cell extracts prepared in detergent solution for the estimation of relative amount of free and bound Cp_6 in cells. The incubation time was fixed as 3 h. The results in Fig. 4.7 & b show that at both the concentrations, there are no significant difference in relative amount of free Cp_6 and its SiNP complex in the cells at 3 h incubation.

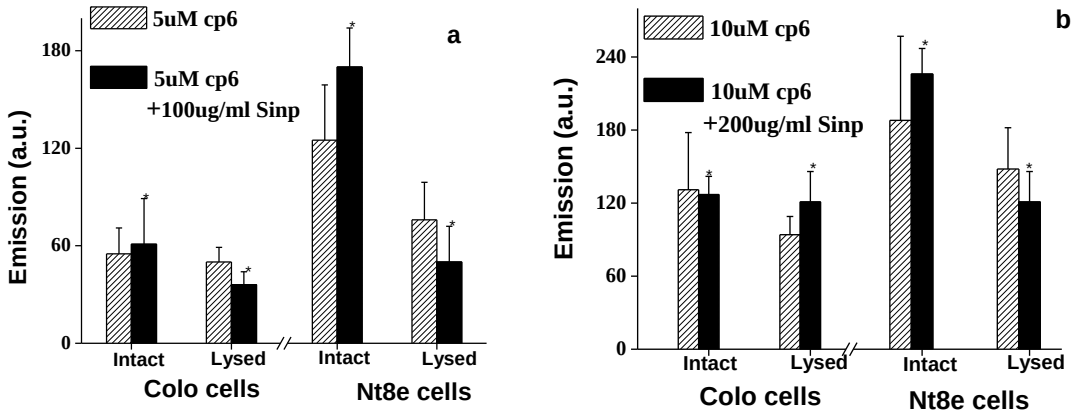

Figure 4.7 *Data showing cellular uptake of Cp_6 as relative fluorescence intensity in intact cells and after extraction in SDS:NaOH solution for Colo-205 and Nt8e cells. The cells were incubated with Cp_6 or Cp_6-SiNP at (a) 5µM Cp_6 and its complex with SiNP at 100 µg/ml and (b) 10 µM Cp_6 and its complex with SiNP at 200 µg/ml. Data are average ± standard deviation of values obtained from three independent experiments. * - Significant ($p < 0.01$).*

Intracellular localization : The fluorescence images of the Colo-205 and NT8e cells taken after 3 hour incubation with free Cp_6 and Cp_6 bound to SiNP are shown in Fig. 4.8. In Colo-205 cells the fluorescence from both free (Fig 4.8a) and SiNP bound Cp_6(Fig

4.8b) can be seen to localize mainly in the cytoplasm. In case of NT8e cells also, the intracellular localization of free Cp_6 and Cp_6-SiNP complex was similar (Fig 4.8 c & d).

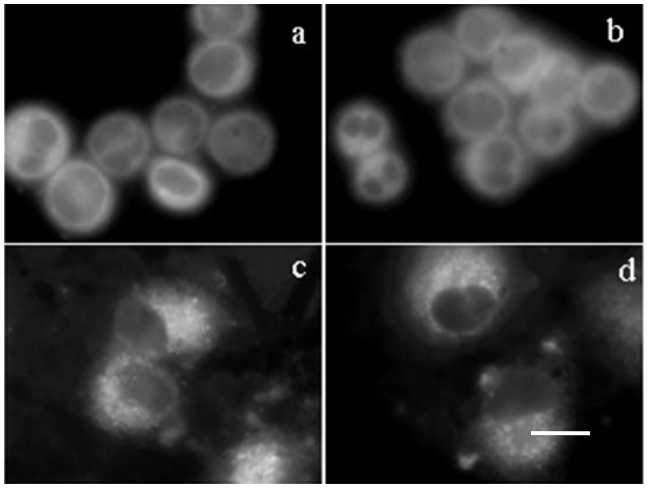

Figure 4.8 *Fluorescence microphotographs of Colo-205 cells (a, b) and Nt8e cells (c-d) showing intracellular localization of Cp_6 (a, c) and Cp_6-SiNP (b, d). Magnification, 100 X, Bar- 25 µm.*

Cytotoxicity: The effect of free Cp_6 and its SiNP complex after 3 h incubation on survival of Colo-205 and NT8e cells, kept in dark and after exposure to red light, is shown in Fig. 4.9a & b. The data are compared with respect to the cell survival of a control sample that received no Cp_6 and no light. It was observed that Cp_6 alone (5 µM and 10 µM) in dark led to 10-15% cytotoxicty indicating slight dark toxic effect. In comparison, Cp_6-SiNP complex alone, at lower concentration (5 µM Cp_6 and 100 µg/ml SiNP), almost the same level of dark toxicity was shown (Fig. 4.9a) whereas upon exposure to red light the phototoxicity was found to increase by ~20-25% (Fig. 4.9a). However, no significant difference is observed in phototoxicity induced by Cp_6-SiNP and free Cp_6 at this lower concentration ($p > 0.05$). At higher concentrations, Cp_6-SiNP conjugate (10 µM Cp_6 and 200 µg/ml SiNP) in dark led to considerable increased cytotoxicity, by ~30-35 % (Fig. 4.9b). This toxicity is mainly due to SiNP since the addition of SiNP alone (200 µg/ml) also led to enhanced cytotoxicity to the same level in both the cell lines (Fig. 4.9b).

Upon exposure to red light, the cells treated with higher concentrations of Cp_6-SiNP, showed increase in phototoxicity by ~85% which was nearly double than the increase in phototoxicty (~40%) induced by 10 µM Cp_6 and light. SiNPs alone in the presence of light showed no significant change in cytotoxicity as compared to SiNP in dark suggesting that SiNP did not contribute to the phototoxicity.

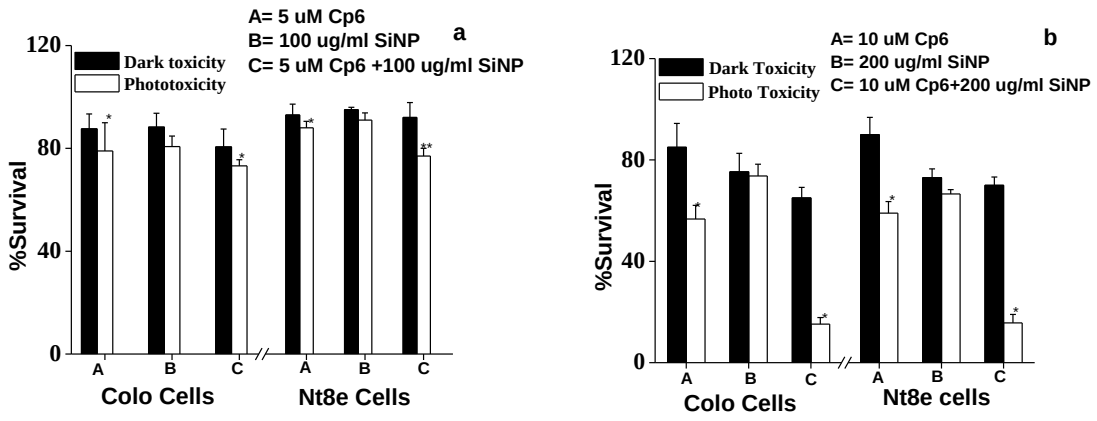

Figure 4.9 *Data showing changes in percent cell survival following photosensitizer treatment in dark and after exposure to light for Colo-205 and Nt8e cells. The cells were incubated with Cp_6 or Cp_6-SiNP at two different concentrations. (a) 5 µM Cp_6 and its complex with SiNP at 100 µg/ml and (b) 10 µM Cp_6 and its complex with SiNP at 200 µg/ml. Data are average ± standard deviation of values obtained from three independent experiments. * - Significant (p < 0.01).*

4.3.4 Relative photo-stability of the free Cp_6 and Cp_6-SiNP complex

The photostability of the Cp_6 and its complex with nanoparticles was monitored by measuring the changes in Soret band absorbance of the free Cp_6 and its SiNP complex after exposure to red light. These experiments were done in aqueous as well as serum (10%) media since the latter environment is more relevant with respect to this work. The plot of change in absorbance (in log scale) of the Cp_6 vs. irradiation time is shown in Fig. 4.10. For all cases a linear decrease in absorbance with increase in irradiation time was observed. In aqueous medium both with and without serum, the photostability of the Cp_6 increased significantly when SiNP were present.

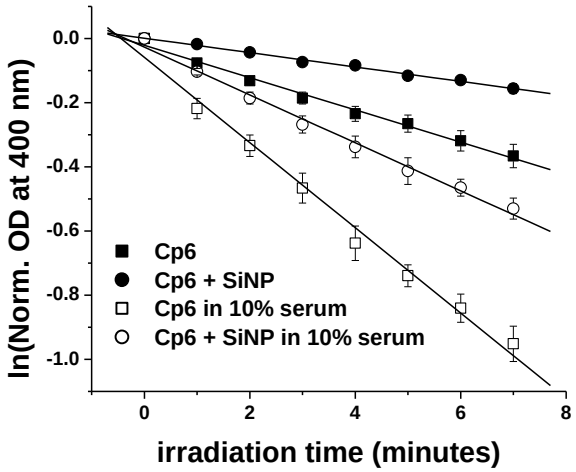

Figure 4.10 *Photobleaching of 10 μM Cp_6 under irradiation at 660 ± 20 nm. The kinetics was followed by monitoring the decrease in the optical density (OD) of the Soret band of the* Cp_6. *(SiNP = 200 μgm/mL)*

4.4 Discussion

A decrease in pH causes successive protonation of the carboxylic groups of Cp_6, which results in the formation of hydrophobic species corresponding to structures C-A in Fig. 4.1 [91]. The aggregation of these hydrophobic species in aqueous medium results in a progressive decrease in the absorbance and fluorescence intensities of the dye. The pH dependent spectroscopic property of the dye in aqueous medium is shown in Fig. 4.2a and c. In the presence of SiNP, this pH dependent spectroscopic property of the dye in aqueous medium is observed to alter significantly (Fig. 4.2b and d & Table 4.1). As the pH is lowered, the change in the intensity of the Soret and Q band is modest as compared to the change in the absence of SiNP (Fig. 4.2). However, it is accompanied by a gradual red shift at Q band. The Q band splits into two bands below pH 5.0. The emission of the dye also decreases to a much lesser extent (~ 1.3 times compared to ~12 times in the absence of SiNPs) and is accompanied by a noticeable red shift of the band maxima. In emission there is an appearance of a second band (~650 nm) as the pH is lowered (below 6.0), which gets prominent as the pH is lowered further and is clearly visible at pH 3.0. In

short till pH 5.0, the absorption and emission properties of the dye in the presence of SiNPs remain more or less unchanged (except the red shift) and below that the Q band and emission splits into two. These observations indicate that SiNPs are affecting the pH dependent acid-base equilibrium of the dye.

The observed changes may be due to the binding between the dye and nanoparticle which may arise due to both electrostatic and hydrophobic interaction. Electrostatic binding is possible at higher pH due to the presence of positively charged 3-amino propyl groups at the surface of the SiNPs and negatively charged carboxyl groups of Cp_6. However, at low pH, hydrophobic binding between the dye (species A-C) and nanoparticle is also a possibility because the interior of these SiNPs are reported to be hydrophobic in nature [45].

At pH 8.0, where the trianionic form of the dye (species D, Fig. 4.1) is the most abundant, electrostatic binding between the dye and SiNP is expected. With the addition of increasing amounts of SiNP the fluorescence intensity and lifetime of the dye passes through a minimum at a SiNP concentration of 19.0 µgm/mL (Fig. 4.3 and Table 4.2). The occurrence of a minima can be explained by the fact that when dye:SiNP ratio is larger (i.e. at low SiNP concentration since concentration of the dye is fixed at 1µM) the intermolecular separation between the dye molecules bound to the SiNP becomes sufficiently small. This induces self quenching of the fluorescence as there is a considerable overlap between the Q-band absorption and emission. It may be noted that similar behavior was observed earlier in the presence of positively charged surfactant CTAB and liposomes [134, 135, 136]. After that both intensity and lifetime increases steadily and at a SiNP concentration of 940 µgm/mL the absorption (Q band) and emission of the dye is red shifted by ~10 nm accompanied by a modest increase (1.25 times) in emission intensity and lifetime (1.2 times) at this pH (Table 4.1 & 4.2). The observed changes in the fluorescence intensity and lifetime of the dye at different SiNP concentrations suggest a strong electrostatic binding between the dye and SiNP at pH 8.0.

At pH 5.0, due to the partial protonation of the carboxylic acid groups, species like A-C will start to form aggregates, which will decrease the absorption and emission of the dye as noted earlier. The observed trend of the dye's fluorescence with increasing amount of SiNP at this pH is quite similar to those observed at pH 8.0 with the exception that here the minima of fluorescence intensity and lifetime occurs at different SiNP concentrations (Fig. 4.4 and Table 4.2). At a SiNP concentration of 940 µgm/mL the absorption (Q band) and emission of the dye is red shifted by ~25 nm accompanied by a 4 times enhancement in emission intensity and 1.4 times enhancement in the lifetime (Table 4.1 & 4.2). The magnitude of the changes observed at this pH is larger than that observed at pH 8.0. We also note from Table 4.1 & 4.2 that the spectroscopic properties like Q and emission band maxima and the lifetime of the dye in the presence of SiNP are quite similar at pH 5.0 and 8.0. These observations suggest that at pH 5.0 and 8.0, the species of the dye that are involved in the binding with SiNP is most likely to be the tri-anionic species (D) of the dye. It may be noted that a similar kind of behavior was observed in earlier studies where the binding of the dye with Cremophor EL at pH 5.0 and pH 7.0 was monitored by fluorescence spectroscopy [138]. The more hydrophilic species of the dye (species D) was observed to get bound preferentially with the hydrophobic Cremophor EL at pH 5.0, which was explained by a hindrance to the protonation of Cp_6 trianionic species caused by Cremophor EL.

At pH 3.0, the absorption and emission of the dye is much weaker because the hydrophobic species are in abundance due to the protonation of the carboxyl groups. However, the aggregation of the dye at this pH is significantly altered in the presence of SiNPs although the observed trend of the dye's fluorescence with increasing amount of SiNP at pH 3.0 is quite different to those observed at pH 5.0 or 8.0. At this pH the Q band of absorption and the emission spectra are clearly splited into two bands (Fig. 4.2d & 4.5a). The presence of two peaks at ~645 and ~670 nm in the synchronous fluorescence spectra of the dye (Fig. 4.5e) suggests that there are two species of the dye at pH 3.0 in

the presence of SiNP. While the species responsible for fluorescence at 645 nm band is seen to be insensitive to SiNP concentration, the species responsible for fluorescence at 670 nm band is sensitive to changes in SiNP concentration (Fig. 4.5 b-d) and its spectroscopic parameters are similar to that observed at pH 5.0 & 8.0 which implies that it is most likely originating from the trianionic form of the dye (species D, Fig. 4.1) bound to SiNP.

The species responsible for fluorescence at 650 nm (with a lifetime of 2.0 ns) could either be due to free dye or dye bound to SiNP. To test this we have studied the effect of a quencher, acrylamide on the dyes fluorescence at this pH in the presence of SiNP. At pH 8.0 and 5.0, we have observed that acrylamide is only effective in quenching the fluorescence of the dye in the absence of SiNP (data not shown). The significant quenching of the fluorescence peak at 650 nm by acrylamide (Fig. 4.5f) suggests that the species emitting at 650 nm is coming from the free dye i.e. not bound to SiNP. The increase in emission intensity and lifetime of the 650 nm peak when approaching highest SiNP concentration as observed in Fig. 4.5a-d is most likely due to the contribution coming from the 678 nm emission. Although the binding between the dye and nanoparticle still remains at pH 3.0, the strength or amount of binding is obviously reduced as compared to pH 8.0 and 5.0 because a significant fluorescence from the unbound dye still persists at this pH. It seems that at this pH the strength of the hydrophobic attraction between the partially protonated species (A-C) competes with that of the electrostatic force of attraction between the negatively charged species (D) and the positively charged SiNP.

These spectroscopic studies show that conjugation of SiNP with Cp_6 modifies the pH dependent equilibrium of the Cp_6. Therefore the PDT efficacy may also get affected as cellular uptake has been shown to be pH dependent [131]. For cellular uptake studies the cells were incubated in growth medium which contains serum proteins. It has been shown earlier that Cp_6 has affinity to bind to the hydrophobic sites of serum proteins

[140]. Therefore, in the growth medium, Cp_6 of the Cp_6-SiNP conjugate has probability to competitively bind to protein or remain bound to the SiNP. The hydrodynamic radii of the free Cp_6 and its complexes with the serum proteins or nanoparticles will be different. As FCS measures hydrodynamic radii of the fluorescent particles and can give a quantitative estimation about the relative association of the Cp_6 with serum proteins and nanoparticles, the relative association of Cp_6 with SiNP and serum proteins was investigated by performing FCS experiments in presence of SiNP with varying amounts of serum. The fitting of the autocorrelation curves against Cp_6-SiNP conjugates in the presence of 10% serum (Fig. 4.6) show two components with probability ratio 20 and 100 corresponding to free and SiNP bound Cp_6 respectively. Thus, results of FCS experiments indicate that the majority of the Cp_6 remains bound to SiNP even in the presence of serum proteins. As similar concentration of serum proteins are found in the cells also, the results suggest that the majority of the Cp_6 remains bound to SiNP even in cells when these cells were incubated with the Cp_6-NP conjugates.

The cellular uptake and phototoxicity of free Cp_6 and Cp_6-SiNP complex were examined in Colo-205 and Nt8e cells. Since the local cellular environment can interfere with the fluorescence yield of the photosensitizer and thus with the estimation of its relative amount, we measured the Cp_6 fluorescence in intact cells as well as in cell extracts prepared in detergent solution. The 3h incubation time was fixed on the basis of a time dependent analysis which showed that while the uptake of Cp_6 increases linearly up to 3 h and then saturates, for Cp_6-SiNP the uptake was found to decrease beyond 3 h possibly because of an increase in dark toxic effect of Cp_6-SiNP at later time points (data not shown).

The results of cellular uptake showed no difference in the relative amount of Cp_6 localized in the cells when it is given as free form or as SiNP complex (Fig. 4.7 a & b). Cellular microscopy studies (Fig.4.8) done in the Colo-205 and NT8e cells lines showed the presence of punctuate pattern of Cp_6 fluorescence in the cytoplasm. However,

the intracellular localization pattern of Cp_6-SiNP in both the cell lines was similar to free Cp_6. Interestingly, while lower concentration of Cp_6-SiNP showed no significant difference in the phototoxic effect as compared to Cp_6, for higher concentrations (10 µM Cp_6 and 200 µg/ml SiNP) the phototoxicity induced by Cp_6-SiNP was much higher than free Cp_6 (Fig**.** 4.9a & b). There was however, considerable dark toxicity due to SiNP alone which also contributed to the dark toxicity of Cp_6-SiNP at higher concentration. SiNP alone has been shown to induce cytotoxicity via induction of oxidative stress in human bronchoalveolar carcinoma-derived cells [129]. Whether such effect can contribute to the observed cytotoxicity of SiNP in Colo-205 and Nt8e cells is presently not clear. However, SiNPs alone in the presence of light showed no significant change in cytotoxicity as compared to SiNP in dark suggesting that SiNP did not contribute to the phototoxicity.

We also measured the photostability of free Cp_6 and Cp_6-SiNP in serum media which is expected to significantly influence its photodynamic efficacy [141]. In aqueous medium, both with and without serum, the photostability of Cp_6-SiNP was found to be higher than the free Cp_6 (Fig. 4.10). The improved photostability of the Cp_6 in the presence of SiNP in serum media is consistent with the results obtained from FCS experiments. Thus, due to the lower rate of photobleaching of Cp_6-SiNP complex, the concentration of the active photosensitizer during the treatment is expected to be higher and this appears to be the main reason for the observed increase in phototoxicity of Cp_6-SiNP complex.

4.5 Conclusion

Our experimental results demonstrate that the pH dependent acid-base equilibrium of Cp_6 in aqueous medium is affected in the presence of SiNP. In the absence of SiNP, the lowering of pH enhances the formation of partially/fully protonated species (Fig. 4.1, A-C) which are hydrophobic in nature and thus form nonfluorescent aggregates. However,

in the presence of SiNPs, these partially or fully protonated species of the dye get bound to SiNP by electrostatic force of attraction. The spectroscopic signature of the dye that is bound to SiNP at pH 5.0 is very similar to that at pH 8.0 and it is suggested that the tri-anionic form of the dye remains bound to the positively charged SiNP at these pH. The presence of electrostatic binding force was observed even at pH 3.0 which competes with intermolecular hydrophobic forces and as a consequence the formation of hydrophobic aggregates at this pH is disrupted significantly. Thus, pH is observed to play a significant role in controlling the binding between the dye and nanoparticle. The formation of a stable dye-nanoparticle complex around physiological pH is expected to affect the relative uptake and photodynamic efficacy of the free dye and the dye-nanoparticle complex in cancer cells. This was investigated using colon and oral carcinoma cell lines. Our study showed that the complex of Cp_6 with SiNPs produced higher phototoxic effect on both the cells as compared to free Cp_6. The intracellular uptake and localization of the free Cp_6 and Cp_6-SiNP complex showed no difference. However, the preferential binding of Cp_6 with SiNP in serum media was confirmed by FCS experiments which could result in an improvement of its photostability. This is suggested as the main reason for the observed increase in the phototoxicity of Cp_6-SiNP. Thus, Cp_6-SiNP was shown to provide better photodynamic efficacy as compared to free Cp_6. It is also expected that SiNP bound Cp_6 would accumulate better in tumors due to EPR effect. At present, one major concern in use this formulation is toxic effect of SiNPs when used at higher concentrations. It is expected that covalent attachment of Cp_6 to SiNP should help reduce the required concentration of SiNP for more efficient drug delivery. Therefore, further investigations in cell culture using covalently coupled Cp_6-SiNP are necessary to prove the potential advantage of such formulation.